Journal of Alloys and Compounds 618 (2015) 527–532

Contents lists available at ScienceDirect

Journal of Alloys and Compounds

journal homepage: www.elsevier.com/locate/jalcom

Crystallography and morphology of antiphase boundary-like structure induced by martensitic transformation in Ti–Pd–Fe alloy

M. Matsuda [a,*], S. Nishimura [a], S. Tsurekawa [a], K. Takashima [a], M. Mitsuhara [b], M. Nishida [b]

[a] *Department of Materials Science and Engineering, Kumamoto University, 2-39-1 Kurokami, Kumamoto 860-8555, Japan*
[b] *Department of Engineering Sciences for Electronics and Materials, Kyushu University, Kasuga, Fukuoka 816-8580, Japan*

A R T I C L E I N F O

Article history:
Received 11 July 2014
Received in revised form 21 August 2014
Accepted 31 August 2014
Available online 10 September 2014

Keywords:
Metals and alloys
Microstructure
Phase transitions
Shape memory
Transmission electron microscopy, TEM

A B S T R A C T

The antiphase boundary (APB)-like structure of both 9R and B19 martensites in the Ti–Pd–Fe alloy was investigated by means of transmission electron microscopy. Some APB-like structures with curved and wide contrasts along the $(0\,0\,1)_{9R}$ basal plane are observed in 9R martensitic plates. The atomic displacement on the APB-like structure reflects the atomic movement stemming from the microdomains formed as a pre-martensitic transformation. The displacement vector of the APB-like structure in the B19 martensite can be expressed as $\boldsymbol{R} = \langle 1/3\,0\,{-1/2}\rangle_{B19}$. The density of APB-like contrasts increases by the substitution of Fe for Pd in Ti–Pd–Fe alloy.

1. Introduction

Near equiatomic Ti–Ni and Ti–Pd alloys undergo thermoelastic martensitic transformation from the B2 to B19′ (monoclinic) and B19 (orthorhombic) structures upon cooling, respectively. The former alloy is a technologically important material with superior shape memory effect and superelasticity [1]. The latter alloy is a candidate for high-temperature shape memory material because its transformation temperature is about 800 K [2]. We have discovered an antiphase boundary (APB)-like contrast of the martensite in Ti–Ni and Ti–Pd shape memory alloys so far [3,4]. We characterized those APB-like structures as a kind of stacking fault with an APB-like morphology that is induced by the martensitic transformation. Recently, Inamura et al. discovered an APB-like contrast in α'' (orthorhombic)-martensite in a Ti–Nb–Al alloy [5]. We also analyzed an APB-like contrast of the B19′ martensite via an R-phase transformation in a Ti–Ni–Fe alloy [6]. It is concluded that the atomic displacement on such contrasts within martensitic variants reflects to the atomic movements stemming from the pre-existing athermal ω-phase and R-phase transformations. All these reports provide the characterization of the APB-like structure in the martensite consisting of simple 2H structures. However, APB-like structure in martensite with long period stacking order (LPSO) structures has not been clarified.

The effect of the substitution of Fe for Pd on the martensitic transformation temperature and structure in Ti–Pd–Fe alloy has been extensively studied [7–12]. The structures of martensite are dependent on Fe content, they are regarded as LPSO structures with common basal planes, that is, 2H, 9R, 4H and their modified structures with incommensutate periodicities. The aim of the investigation reported here is to clarify the crystallography and morphology of the APB-like structure of the 9R martensite, which is one of the LPSO structures in Ti–Pd–Fe alloy, by means of conventional transmission electron microscopy (CTEM) and high-resolution transmission electron microscopy (HRTEM). Furthermore, high-angle annular dark-field scanning transmission electron microscopy (HAADF-STEM) is applied to analyze the interface structure at the atomic level, by which the relatively heavy atom positions are identified by bright contrast in the image due to atomic number (Z) contrast [13,14]. The effect of substitution of Fe on the APB-like structure in Ti–Pd–Fe alloy is also discussed on the basis of these observations.

2. Experimental procedure

$Ti_{50}Pd_{46}Fe_4$ and $Ti_{50}Pd_{43}Fe_7$ alloys were prepared from 99.7% Ti, 99.8% Pd, and 99.5% Fe (mass%) by arc melting in an argon atmosphere. A $Ti_{50}Pd_{50}$ alloy was also fabricated as a specimen for comparison. The samples were solution treated in an argon atmosphere at 1273 K for 3.6 ks and then quenched in ice water. The transformation temperature to the martensite (Ms) of $Ti_{50}Pd_{46}Fe_4$ and $Ti_{50}Pd_{43}Fe_7$ alloys measured by differential scanning calorimetry were about 690 K and 513 K, respectively, which are in good agreement with those reported previously [8]. The TEM specimens were electropolished to perforation in a Tenupol-3 operated at 12 V,

---

[*] Corresponding author. Tel.: +81 96 342 3718; fax: +81 96 342 3710.
E-mail address: matsuda@alpha.msre.kumamoto-u.ac.jp (M. Matsuda).

http://dx.doi.org/10.1016/j.jallcom.2014.08.258
0925-8388/

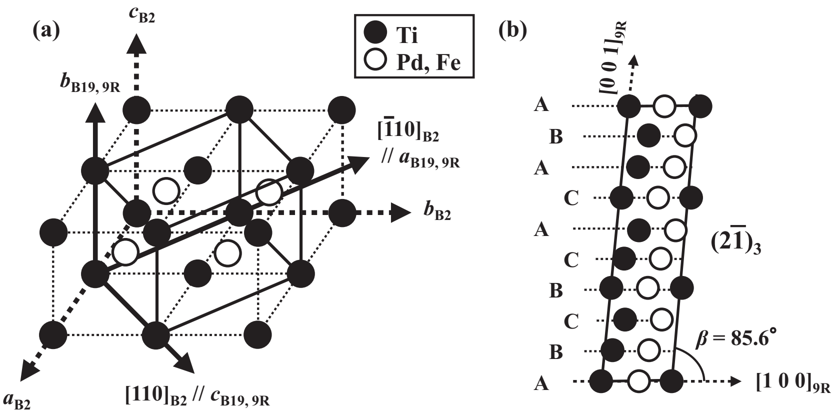

Fig. 1. (a) Lattice correspondence between the B2 parent phase, the B19 and 9R martensite. Dashed lines indicate the B2 structure, and solid lines show the B19 and 9R structures, respectively. (b) Schematic illustration of the unit cell of 9R structure.

0.03 A, and 273 K in an electrolyte solution consisting of glacial acetic acid; 72%, methanol; 12%, ethylene glycol; 8% and perchloric acid; 8% by volume. CTEM and HRTEM observations were carried out with JEM-2000FX and FEI-Tecnai20F microscopes, respectively, which were both operated at 200 kV. The HAADF-STEM observation was performed by JEM-ARM200F (Cs-corrected 200 kV STEM). The electron probe size and current were 0.10 nm and approximately 20 pA, respectively. For the HAADF-STEM images, the annular detector was set to collect electrons scattered at angles between 90 and 170 mrad. The relationship between B2, B19, and 9R are illustrated schematically in Fig. 1 [8]. The following lattice parameters were used for the analysis of the B19 martensite: $a_{B19} = 0.489$ nm, $b_{B19} = 0.281$ nm and $c_{B19} = 0.456$ nm [15], and the 9R martensite: $a_{9R} = 0.467$ nm, $b_{9R} = 0.286$ nm, $c_{9R} = 2.053$ nm, and $\beta = 85.6°$ [8], respectively.

3. Results and discussion

Fig. 2a and b shows the typical bright-field image and electron diffraction pattern taken from the area marked B in (a) in $Ti_{50}Pd_{43}Fe_7$ alloy, respectively. The pattern in Fig. 2b consists of reflections along the $[0\,1\,0]_{9R}$ zone axis, which is a low-index zone axis parallel to the basal plane of martensite with a LPSO structure. We can recognize easily that there is 9R martensite in the area B, since diffraction spots at "1/3" position are seen along the row of $00l^*$ reflections in the pattern, as indicated by the double arrows in Fig. 2b, which can be indexed consistently with the lattice parameter of 9R martensite mentioned above. It is notable that many line and curved contrasts are observed within the twin plates in Fig. 2a. In order to analyze these defects CTEM observations were carried out by using various reflections observed in the $[0\,1\,0]_{9R}$ incidence of electron. HRTEM observations were also performed along this zone axis, as described below, because the atomic columns of Ti and Pd and/or Fe in the 9R structure can easily be distinguished.

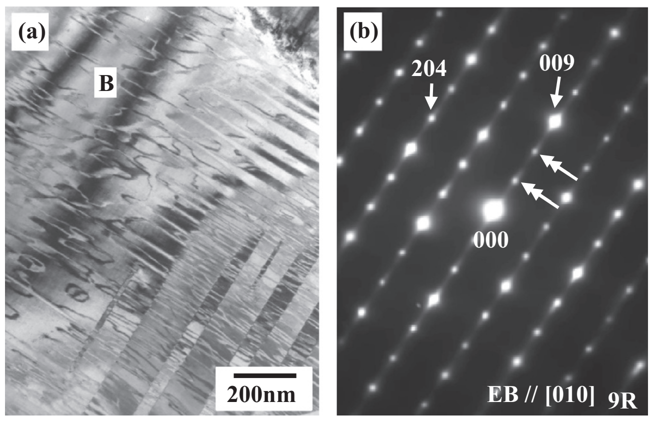

Fig. 2. (a) Bright-field image of a $Ti_{50}Pd_{43}Fe_7$ alloy. (b) Electron diffraction pattern taken from area B in (a).

Fig. 3a and b shows the bright-field image and corresponding electron diffraction pattern, respectively, of the $[0\,1\,0]_{9R}$ zone axis. Some APB-like structures with curved and wide contrasts along the $(0\,0\,1)_{9R}$ basal plane are observed in martensitic plates of the $Ti_{50}Pd_{43}Fe_7$ alloy, as indicated by the arrows in Fig. 3a, whereas APB-like structures with thin linear contrasts along the basal plane are observed in large martensitic plates of the $Ti_{50}Pd_{50}$ alloy, as discussed in our previous report [4]. Fig. 3c and d shows dark-field images taken using $\bar{1}\,0\,1^*_{9R}$ and $\bar{2}\,0\,2^*_{9R}$ reflections, respectively. It has been widely recognized that π contrast of the APB induced by order–disorder transformations can be observed using superlattice reflections for the ordered structure, whereas no contrast is observed using fundamental reflections. The APB-like contrast is observed when both the $\bar{1}\,0\,1^*_{9R}$ superlattice and $\bar{2}\,0\,2^*_{9R}$ fundamental reflections for the 9R structure are used, as shown in Fig. 3c and d. Here, present classification for each superlattice and fundamental reflection in 9R structure follows that proposed by Tadaki et al. [16]. The APB-like contrasts are also observed using 204^* fundamental reflections, although the micrographs are not included here. These facts indicate that the APB-like contrast does not correspond to π contrast; they do, however, correspond to stacking faults with an APB-like morphology induced by the martensitic transformation, as expected from the APB-like structure in Ti–Ni and Ti–Pd alloys [3,4]. It is noteworthy that APB-like contrasts are faintly observed on using the $0\,0\,9^*_{9R}$ reflection corresponding to the $\{1\,1\,0\}_{B2}$ plane, as indicated by the double arrows of Fig. 3e, although no contrast is observed when using the $0\,0\,2^*_{B19}$ reflection corresponding to the $\{1\,1\,0\}_{B2}$ plane in the $Ti_{50}Pd_{50}$ alloy [4]. This phenomenon will be discussed later.

In order to analyze the APB-like contrast at the atomic level, HRTEM observations were carried out along the $[0\,1\,0]_{9R}$ zone axis. Fig. 4a shows the two-dimensional lattice image of the APB-like structure. We can identify the shift of bright spots along the $(0\,0\,1)_{9R}$ plane, as shown by the arrows of Fig. 4a. However, it is difficult to determine the exact location of APB-like boundary by the shift of bright spots along $(1\,0\,0)_{9R}$ plane because the APB-like structure in the $Ti_{50}Pd_{43}Fe_7$ alloy does not show any sharp interface structure, as compared with the two-dimensional lattice image around the APB-like interface in $Ti_{50}Pd_{50}$ binary alloy of Fig. 4b. This indicates that the APB-like interface with such a contrast in the $Ti_{50}Pd_{43}Fe_7$ alloy is not perpendicular but rather tilted with respect to the direction normal to the foil. That is to say, the APB-like contrast in the present $Ti_{50}Pd_{43}Fe_7$ alloy has a displace-